Molecular Therapy
Methods & Clinical Development
Original Article

AAV Gene Therapy Utilizing Glycosylation-Independent Lysosomal Targeting Tagged GAA in the Hypoglossal Motor System of Pompe Mice

Brendan M. Doyle,[1,6] Sara M.F. Turner,[1,6] Michael D. Sunshine,[1,6] Phillip A. Doerfler,[2,3] Amy E. Poirier,[5,6] Lauren A. Vaught,[2,3,6] Marda L. Jorgensen,[2] Darin J. Falk,[2,3,6] Barry J. Byrne,[2,3,6] and David D. Fuller[1,4,6]

[1]Department of Physical Therapy, University of Florida, Gainesville, FL 32610, USA; [2]Department of Pediatrics, University of Florida, Gainesville, FL 32610, USA; [3]Powell Gene Therapy Center, University of Florida, Gainesville, FL 32610, USA; [4]Mcknight Brain Institute, University of Florida, Gainesville, FL 32610, USA; [5]Department of Neuroscience, University of Florida, Gainesville, FL 32610, USA; [6]Center for Respiratory Research and Rehabilitation, University of Florida, Gainesville, FL 32610, USA

Pompe disease is caused by mutations in the gene encoding the lysosomal glycogen-metabolizing enzyme, acid-alpha glucosidase (GAA). Tongue myofibers and hypoglossal motoneurons appear to be particularly susceptible in Pompe disease. Here we used intramuscular delivery of adeno-associated virus serotype 9 (AAV9) for targeted delivery of an enhanced form of GAA to tongue myofibers and motoneurons in 6-month-old Pompe (*Gaa*$^{-/-}$) mice. We hypothesized that addition of a glycosylation-independent lysosomal targeting tag to the protein would result in enhanced expression in tongue (hypoglossal) motoneurons when compared to the untagged GAA. Mice received an injection into the base of the tongue with AAV9 encoding either the tagged or untagged enzyme; tissues were harvested 4 months later. Both AAV9 constructs effectively drove GAA expression in lingual myofibers and hypoglossal motoneurons. However, mice treated with the AAV9 construct encoding the modified GAA enzyme had a >200% increase in the number of GAA-positive motoneurons as compared to the untagged GAA ($p < 0.008$). Our results confirm that tongue delivery of AAV9-encoding GAA can effectively target tongue myofibers and associated motoneurons in Pompe mice and indicate that the effectiveness of this approach can be improved by addition of the glycosylation-independent lysosomal targeting tag.

INTRODUCTION

Pompe disease is a neuromuscular disorder caused by mutations in the gene encoding the lysosomal glycogen-metabolizing enzyme, acid-alpha glucosidase (GAA), resulting in extensive intracellular lysosomal glycogen accumulation and disruption of cellular architecture and function.[1] Respiratory muscles and motoneurons are particularly susceptible to pathology in Pompe disease.[1] In addition to the diaphragm (phrenic) motor system,[2] the tongue (hypoglossal, XII) motor system can also be substantially impaired in Pompe disease. Tongue weakness and macroglossia are associated with difficulty feeding, swallowing, breathing, and speaking and a high prevalence of obstructive sleep apnea.[3–6] Studies in Pompe mice (*Gaa*$^{-/-}$) indicate that XII motoneurons develop signs of histopathology early in disease progression.[7] Pompe disease pathology can impact motor control at multiple levels including muscle fibers,[8,9] neuromuscular junctions,[10] nerve fibers,[10] and motoneurons.[2] Therefore, effective treatments for primary respiratory and/or airway-related dysfunction should target the entire motor unit.[1] The current FDA-approved therapeutic strategy is lifelong, repeated intravenous infusion of recombinant human GAA (rhGAA), termed enzyme replacement therapy (ERT). This approach can improve survival rate[11] in early-onset patients with modest benefit to the respiratory system.[12,13] In both infantile[12] and late-onset[13] disease, ERT can attenuate respiratory deficits, but many patients eventually require ventilator support. The limited effectiveness of ERT may derive from the inability of the rhGAA enzyme to cross the blood brain barrier,[3] as well as inefficient rhGAA enzyme receptor-mediated uptake and trafficking.[14,15]

The *Gaa*$^{-/-}$ mouse recapitulates many aspects of the clinical Pompe disease phenotype including glycogen accumulation in cardiac and skeletal muscle[16] and motoneurons.[2,7,10] Recent work in the *Gaa*$^{-/-}$ mouse indicates that intramuscular delivery of adeno-associated virus serotype 9 (AAV9) can drive GAA transgene expression in the entire motor unit.[17,18] Specifically, intralingual injection of AAV9 coding rhGAA resulted in GAA expression with partial reversal of histopathology in the tongue and XII motoneuron pool.[18] However, the intralingual injection transduced only a subset of the XII motor pool, and untreated motoneurons showed a classic neurodegenerative phenotype.[18] Potential explanations for the relative low "correction" of XII motoneurons include limited uptake and/or intracellular trafficking of GAA due to the low binding affinity for the cation-independent mannose-6-phosphate receptor (CI-MPR).[14] The CI-MPR is the primary enzyme trafficking agent for ERT,[19,20] and delivery of rhGAA to the lysosome can be enhanced by tagging the enzyme with a high-affinity CI-MPR ligand.[14] This is accomplished by fusing

Received 6 June 2019; accepted 23 August 2019;
https://doi.org/10.1016/j.omtm.2019.08.009.

Correspondence: David D. Fuller, Department of Physical Therapy, University of Florida, Gainesville, FL 32610, USA.
E-mail: ddf@phhp.ufl.edu

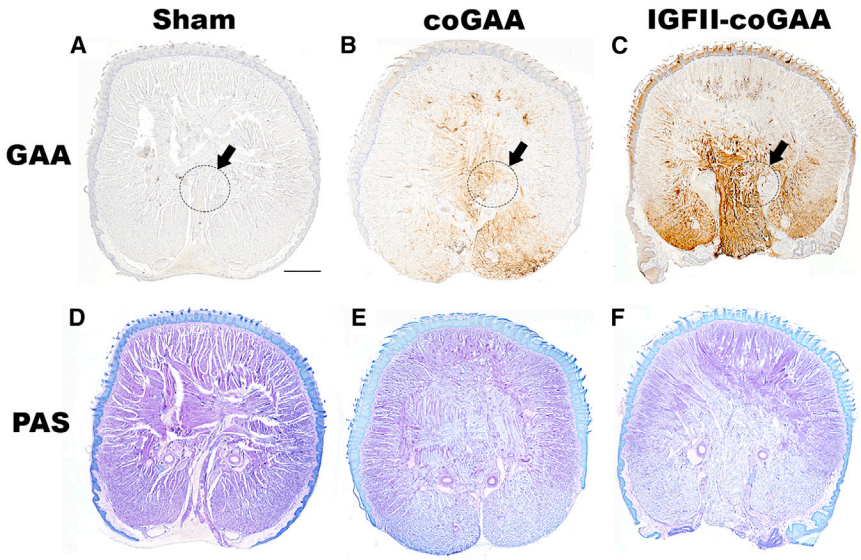

Figure 1. GAA Immunostaining Corresponds to Absence of PAS Stain

(A–F) Adjacent tissue sections from the body of the *Gaa*$^{-/-}$ mouse tongue were stained to recognize GAA (A–C) or glycogen (D–F). Following sham treatment (A and D), tongue histology indicates a complete absence of GAA with glycogen accumulation throughout the tongue. Following treatment with AAV9-DES-IGFIIcoGAA (B and E) or AAV9-DES-coGAA (C and F), GAA immunostaining is evident and corresponds to an absence of PAS staining, indicating clearance of glycogen. The arrow and circle highlights the approximate location of the AAV9 or sham injections. Scale bar, 500 μm.

the N-terminus of the rhGAA protein with a peptide-based glycosylation-independent lysosomal targeting (GILT) tag.[14] In addition to improved intracellular trafficking, if GAA is secreted by a transduced cell, then the IGFII tag allows for more efficient intercellular trafficking by utilizing the IGFII-M6P coreceptor for uptake by surrounding cells.[15,21]

In the current study we used an AAV9 encoding a GILT-tagged GAA (specifically an IGFII-codon optimized human GAA [coGAA] fusion protein) for targeted gene therapy of the XII motor system in *Gaa*$^{-/-}$ mice. Our purpose was to compare and contrast the ability of an AAV9-Desmin (DES)-IGFIIcoGAA construct with an AAV encoding a non-GILT-tagged GAA (AAV9-DES-coGAA)[10] to drive GAA expression in tongue myofibers and XII motoneurons. Based on *in vitro* studies of the GILT tag,[14] we hypothesized that intralingual administration of the AAV9-DES-IGFIIcoGAA vector would more effectively drive GAA expression and cellular uptake. The AAV vector used here drove the expression of coGAA, meaning that rare codons are replaced to match the most prevalent tRNAs, an approach that can increase protein synthesis rates.[22] We focused the analyses on GAA expression in XII motoneurons because of the emerging appreciation of the role of neuropathology in Pompe motor dysfunction. Motoneuron pathology is well established in animal models of Pompe disease,[7,23] and recent reports in humans highlight the importance of the central nervous system in Pompe.[2,24–26] The results of the current study confirm that targeted lingual delivery of AAV9-GAA can treat neuromuscular pathology and indicate a GILT-tagged GAA vector cassette more effectively drives XII motoneuron GAA expression.

RESULTS

Tongue Histology and GAA Activity

Immunohistochemistry confirmed an absence of GAA in tongues of sham-treated *Gaa*$^{-/-}$ mice (Figure 1A). This was associated with glycogen accumulation as indicated by Periodic Acid Schiff (PAS) staining throughout the tongue (Figure 1D). Conversely, GAA immunostaining was prominent in the lingual myofibers of *Gaa*$^{-/-}$ mice following treatment with either of the AAV9 vectors (Figures 1B and 1C). The treated mice also had an absence of PAS staining in tongue myofibers at and around the site of injection (Figures 1E and 1F). Figure 2 illustrates that positive GAA staining after AAV9 treatment was associated with an absence of histopathology in tongue myofibers. Vacuolization and PAS staining are prominent in sham-treated myofibers but are largely absent following either AAV9 treatment (Figure 2).

Figure 3A provides a three-dimensional reconstruction of a tongue following AAV9 injection. The three-dimensional image shows GAA and PAS staining and was created using serial histological sections from the anterior to posterior tongue (e.g., Figure 3B). Note the inverse relationship between GAA expression and PAS positivity—this was observed in all tongues treated with AAV9. The anterior (tip) of the tongue was typically positive for PAS, but PAS staining diminished (and GAA expression increased) as the sections progressed posteriorly to the base of the tongue (site of the AAV9 injection) Thus, the single AAV9 injection to the tongue base (20 μL, 1e10 vector genomes [vg]) did not drive GAA expression across the length of the tongue but was highly effective in driving GAA expression in a 2–3 mm region near the base.

The activity of the GAA enzyme was measured in whole tongue muscle homogenates. The enzyme activity data were not normally distributed and were statistically evaluated using a one-way ANOVA on ranks. Figure 4 illustrates an overall difference in median values across the four experimental groups ($p = 0.006$). Wild-type (WT) tongues had activity levels of 42 ± 4 nmol/h/mg and sham-treated *Gaa*$^{-/-}$ tongues had values of 1.4 ± 0.7. Both AAV9 vectors substantially increased lingual GAA activity with values reaching 207 ± 27% of WT following AAV9-DES-IGFIIcoGAA treatment and 366 ± 52% of WT after AAV9-DES-coGAA. Both the AAV9-DES-coGAA ($p = 0.009$) and AAV9-DES-IGFIIcoGAA ($p = 0.012$) treated *Gaa*$^{-/-}$ tongues had statistically greater GAA activity as compared to the sham-treated *Gaa*$^{-/-}$ tissues.

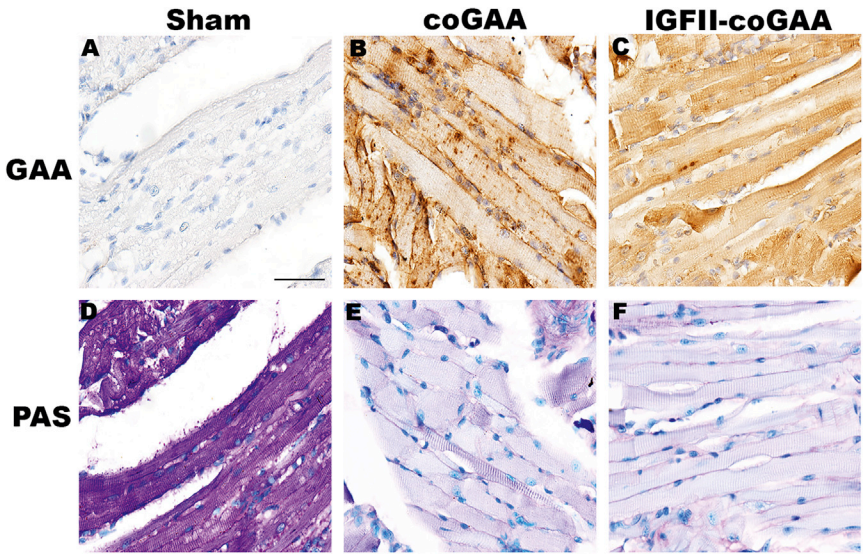

Figure 2. Tongue Histology after Sham or AAV9-GAA Therapy

(A–F) Tissues from *Gaa*$^{-/-}$ mice were stained to recognize GAA (A–C) or glycogen (PAS) (D–F). Following a sham tongue injection, myofibers (A and D) demonstrate the prototypical vacuolated appearance associated with Pompe disease. Tongue tissues treated with AAV9-DES-IGFIIcoGAA (B and E) or AAV9-DES-coGAA (C and F) stain positive for GAA and do not have the vacuolated appearance. Scale bar, 30 μm.

XII Nerve Histology

Histological sections from sham-treated *Gaa*$^{-/-}$ mice had positive PAS staining throughout the nerve, consistent with prior reports.[10] As shown in Figure 5, PAS staining can be readily observed throughout the sham-treated XII nerve. Both AAV9-GAA treatment paradigms appeared to have an impact as shown by less prominent PAS staining (purple globules) in *Gaa*$^{-/-}$ XII nerve sections (Figure 5). The bottom panels of Figure 5 highlight representative 50 μm^2 areas of XII nerves from each treatment group. Note that distinct clusters (purple globules) of positive PAS staining can be seen in the sham-treated tissue, whereas the AAV-GAA groups have a lower density of glycogen accumulations.

GAA Expression in XII Motoneurons

Consistent with published anatomical descriptions,[27] the XII nucleus could be clearly identified in all mice as shown in Figure 6. Motoneurons were identified based on location, size, and morphology. In sham-treated *Gaa*$^{-/-}$ mice, XII motoneurons demonstrated the prototypical Pompe histopathology including a swollen, vacuolated appearance.[7,18] Immunostaining for GAA was absent throughout the medulla and XII motoneurons were uniformly PAS positive in sham-treated *Gaa*$^{-/-}$ mice. Lingual delivery of either AAV9 vector resulted in GAA expression in a subset of XII motoneurons (Figure 6). When GAA expression was immunohistologically detected in XII motoneurons, these same motoneurons had an apparent reversal of the typical Pompe histopathology. This is illustrated by directly comparing GAA-positive motoneurons that happen to be juxtaposed with GAA-negative motoneurons. Thus, as shown in Figure 7, GAA-positive cells are PAS negative and lack the swollen and vacuolated appearance of the adjacent GAA-negative motoneurons.

In both AAV9 treatment groups, GAA-positive XII motoneurons could be identified throughout the rostral-caudal axis of the XII motor nucleus as illustrated in Figure 8. Morphologically, GAA-positive XII motoneurons of both treatment groups appear similar (Figure 6), indicating a similar treatment efficacy produced by either vector when present. Quantitative evaluation of GAA-positive cells indicated that the AAV9-DES-IGFIIcoGAA administration was more effective at driving GAA expression (Figure 8). This difference was most apparent in the caudal aspect of the XII nucleus (Figure 8). Overall, *Gaa*$^{-/-}$ mice treated with AAV9-DES-coGAA showed an average of 59 ± 10 GAA-positive XII motoneurons, while the AAV9-DES-IGFIIcoGAA treatment group showed an average of 185 ± 24 GAA-positive motoneurons ($p < 0.008$, unpaired t test).

DISCUSSION

Our results confirm that intralingual delivery of AAV9-GAA can effectively drive GAA expression in tongue myofibers and XII motoneurons. Persistent GAA expression was accompanied by clearance of glycogen and restoration of normal cellular morphology in lingual myofibers and XII motoneurons. Accordingly, it may be possible to selectively target lingual dysfunction in Pompe disease using an intralingual AAV9 delivery approach. The results also indicate that fusion of an IGFII GILT tag to the GAA transgene product enhances GAA expression in XII motoneurons.

Lingual Myofibers and XII Axons

Correction of myofiber histopathology in *Gaa*$^{-/-}$ mice following AAV-GAA therapy is consistent with previous reports.[8,9,17,28,29] Lingual myofibers treated with either of the vectors showed areas of positive GAA staining which were mirrored by an absence of PAS staining. The positive GAA staining coupled with negative PAS staining provides strong evidence that the GAA enzyme produced following intralingual administration of AAV9-GAA causes lingual glycogen clearance.[18] However, lingual myofibers in the anterior tongue remained GAA negative 4 months post-injection of either AAV9-GAA vectors. This is an indication that a single bolus injection of AAV9-GAA (6.5 μL of 1e10 vg, diluted to 20 μL in lactated ringers [LRs]) to the base of the tongue is insufficient to treat the entire length of the murine tongue. Separate AAV9-GAA injections to both the anterior and posterior portions of the tongue are likely needed to drive GAA expression throughout the tongue.

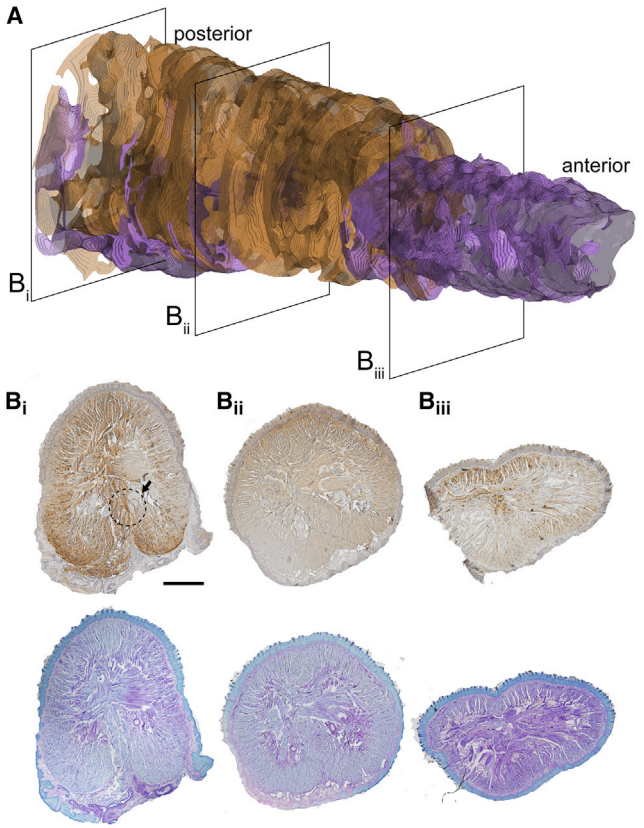

Figure 3. Three-Dimensional Reconstruction of a *Gaa*$^{-/-}$ Mouse Tongue following AAV9-DES-IGFIIcoGAA Treatment

(A and B) Tissue sections spaced 7 μm apart were alternately stained for PAS or GAA across the anterior-posterior axis of the tongue. The reconstruction image (A) was done using photomicrographs (as shown in B) using a MATLAB code (see Materials and Methods). (A) Illustrates that GAA staining is prominent in the posterior 2/3 of the tongue but does not extend to the anterior tip. The bottom panels (Bi–Biii) show photomicrographs of GAA and PAS staining from the cross sectional location indicated in (A). The arrow and circle in (Bi) highlight the approximate location of the AAV9 injection. Scale bar, 500 μm.

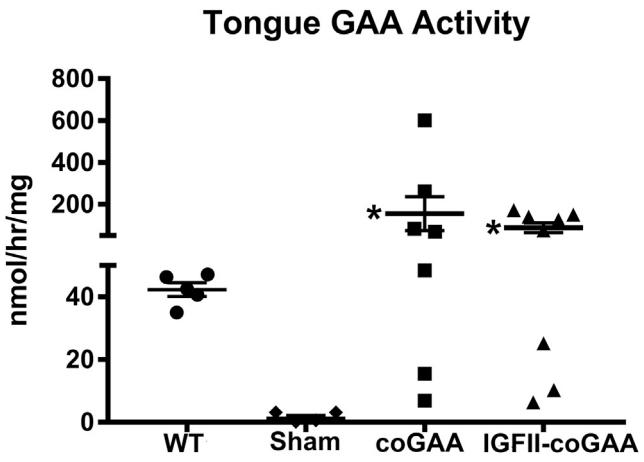

Figure 4. GAA Enzymatic Activity in the Tongue Is Increased after AAV9-GAA Therapy

Untreated knockout (KO) mice show the expected reduction in tongue GAA activity as compared to wild-type (WT). Both of the AAV9 vectors shifted the distribution of GAA activity away from the KO values, with the mean activity exceeding WT levels. A Kruskal-Wallis one-way ANOVA on ranks indicated a statistical difference in the median values across the treatment groups (*p = 0.006). Pairwise multiple comparison procedures using Dunn's Method showed that the AAV9-DES-IGFIIcoGAA group (n = 8; *p = 0.009) and AAV9-DES-coGAA group (n = 7; *p = 0.012) were statistically different than sham treated (n = 5; indicated by * on the figure). The WT sample was n = 5. Error bars indicate SEM.

Biochemical assays verified that the lingual AAV9 injections were effective in driving GAA enzyme activity in the tongue, although variability in the relative amount of GAA activity occurred across animals. One factor contributing to this variability could be the complex architecture of the tongue muscles. The tongue is a multifaceted structure made up of seven different muscles, which are highly interwoven. This creates an environment in which the fluid bolus may diffuse unevenly or differently from one injection to the next. In addition to the highly complex organization of the tongue myofibers, the tongue is a hydrostat and as such the amount of fluid in the tongue at the time of injection and the movement of this fluid caused by muscle contraction could impact diffusion of the fluid bolus. These basic anatomical features of the tongue may make it a more challenging muscular target when compared to muscles such as the tibialis anterior or gastrocnemius, both of which have been injected with similar AAV9-GAA vectors.[10] Those skeletal muscles have a less complex architecture compared to the tongue and have shown more consistent GAA expression following injection of AAV9-GAA.[10]

Tissue sections from the XII nerve of *Gaa*$^{-/-}$ mice had substantial glycogen deposition as has been reported previously for the *Gaa*$^{-/-}$ mouse phrenic nerve.[10] Consistency of the pathological appearance of respiratory-related nerve fibers across studies indicates that this is a common feature of the *Gaa*$^{-/-}$ model. Disruption of nerve morphology may disrupt axonal conduction and contribute to reduced respiratory motor output as reported in prior studies of the *Gaa*$^{-/-}$ mouse.[2]

Targeting XII Motoneurons via Intralingual AAV9 Delivery

In the current study, a single, direct injection to the base of the tongue with AAV9-GAA (1×10^{10} vg) resulted in persistent GAA expression in XII motoneuron somata. Expression of GAA in XII motoneurons following intralingual AAV9 can be explained by retrograde movement of the AAV9 vector particles via the motor axons of the XII nerve. Expression of GAA in the XII motor nucleus was restricted to this focal region and therefore cannot be explained by non-specific AAV9 movement through the vasculature. The current data and prior studies[17,18,30–32] confirm that AAV9 can be effective for the delivery of transgenes to motor pools following intramuscular delivery.

We found an average transduction of 185 and 59 XII motoneurons in the AAV9-DES-IGFIIcoGAA and AAV9-DES-coGAA groups, respectively. Considering that the estimated total number of motoneurons in the XII nucleus has been reported to range from 974[33]

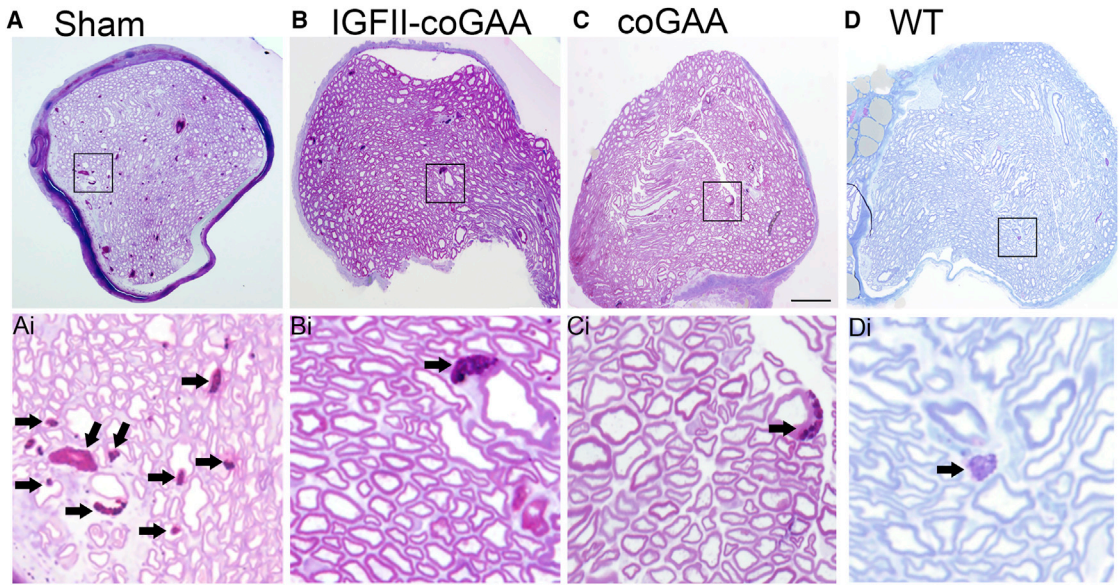

Figure 5. XII Nerve Sections Reveal Glycogen Deposits

(A–D) Nerve samples were plastic embedded, sectioned at 1 μm, and stained with PAS to recognize glycogen. Positive PAS staining is indicated by the distinct "globules" as shown by the arrows in the lower panels. PAS-positive globules can be visualized throughout the tissue section from the sham-treated *Gaa*$^{-/-}$ mouse (A). PAS-positive staining can still be found in nerve sections from AAV9-DES-IGFIIcoGAA (B) and AAV9-DES-coGAA (C) treated XII nerves, although qualitatively the PAS staining appears to be reduced as compared to sham treatment. (D) WT tissues demonstrate less glycogen staining than both sham and treated groups, indicating treatment was insufficient to restore WT glycogen levels. The lower panels provide an expanded view of the area indicated by the black box in the top panels. Scale bar, 50 μm.

to ~1,600[34] in adult mice, this indicates a transduction efficiency of ~12%–19% and ~4%–6%, respectively. The reason for the relatively low retrograde transduction efficacy may relate to the intralingual delivery method. Intramuscular injection results in uptake of viral particle by myofibers and thus reduces the number of viral particles available to move retrogradely.[35] In addition, the tongue histology indicated that GAA expression was primarily restricted to the base of the tongue (e.g., Figure 2). The total number of XII motoneurons expressing GAA would be increased if additional AAV injections were made to the anterior (tip) of the tongue. The estimate of XII motoneuron transduction efficacy may also have been influenced the histological methods. Our histological examination of the XII nucleus was performed every 42 μm, and because the average murine XII motoneuron is between 20–30 μm in diameter[36] it is possible that a percentage of XII motoneurons expressing GAA were not represented. If this is the case, the actual transduction efficiency may have been higher than our 4%–19% estimate. A final consideration is that the functional identity of the transduced XII motoneurons in our study is not known. The XII motor nucleus is somatotopically organized, with intrinsic and extrinsic tongue muscle motoneurons in distinct regions. Of the extrinsic muscle motoneurons, genioglossus motoneurons are found in the caudal aspect of the ventral compartment of the XII nucleus.[37] It may be that a (relatively) larger portion of the genioglossus (or other extrinsic tongue muscles) were transduced by the targeted injection site at the base of the tongue near the insertion point of these muscles. In the current estimate of transduction efficiency, we used published estimates for the entire XII motor pool as the denominator.[33,34] It would be useful, in future work, to evaluate the relative transduction of XII motoneurons associated with specific tongue muscles (e.g., genioglossus, hyoglossus, etc.). However, the complex architecture of the tongue makes selective AAV9 delivery to specific tongue muscles a challenge.

When comparing the two AAV9 recipient groups, the apparent difference in the total number of XII motoneurons expressing GAA may reflect several different mechanisms. First, it is possible that the AAV9-DES-IGFIIcoGAA virus was more efficient at retrograde movement as compared to the AAV9-DES-coGAA virus. We suggest that this explanation is unlikely, however, due to the structural consistency of the AAV9 viral capsids. Castle et al.[38] elucidated the retrograde mechanism of AAV9, in which AAV9 is trafficked into nonmotile early and recycling endosomes, exocytic vesicles, and a retrograde-directed late endosome/lysosome compartment. Retrograde transport of AAV within these endosomes is driven by cytoplasmic dynein and requires Rab7 function.[38] In fact Rab-7 positive late endosomes/lysosomes containing AAV show higher motility with faster retrograde velocities than those without AAV.[38] The mechanism of retrograde movement of AAV9 is conserved in serotypes AAV1 and AAV8.[39] Other viruses, such as the rabies virus, also take advantage of retrograde transport.[40] Once the rabies virus enters the axon, viral P protein binds to the dynein protein DYNLL1, allowing the viral particles to travel along the axon to the neuronal cell body.[40] Like AAV, rabies viral particles are transported within host cells via endosomal transport.[41] This commonality of transport

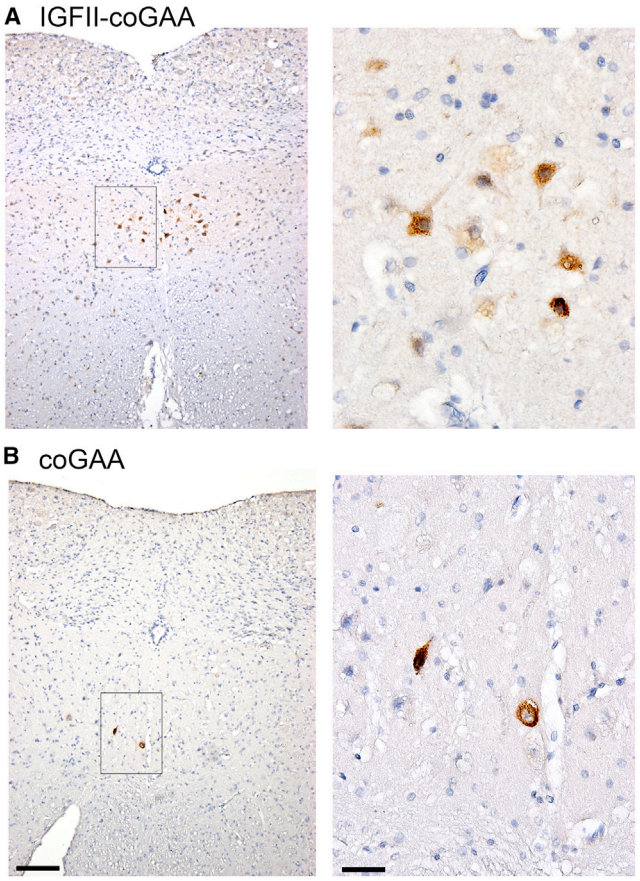

Figure 6. Photomicrographs Depicting GAA-Positive Motoneurons in the XII Nucleus of *Gaa*$^{-/-}$ Mice after Tongue Injection with AAV9-GAA

(A and B) Both AAV9-DES-IGFIIcoGAA and AAV9-DES-coGAA resulted in GAA expression in XII motoneurons. These representative images, taken from the caudal portion of the XII nucleus, illustrate that IGFIIcoGAA treatment (A) was associated with more GAA-positive motoneurons as compared to coGAA (B). The GAA-positive XII motoneurons of both AAV9 groups were morphologically similar. Scale bars, 500 μm (left panels) and 80 μm (right panels).

mechanism may indicate that AAV9 utilizes dynein in a similar fashion for retrograde transport. Uptake of the viral vectors into host cells is also attributable to interactions between the viral capsids and the host cell membrane including endocytosis or membrane fusion.[29] Both vectors had AAV9 capsids, and the same lingual injection method was used for both vectors. The difference between the vectors is that the transgene product would not be expressed until transcription and translation occurs within host cells. Thus, differences in retrograde transport and transduction of host cells are unlikely to be related to transduction efficiency. Several plausible mechanisms to explain the apparent difference in GAA protein expression between the two vectors are discussed next.

Increased efficiency of enzyme trafficking within transduced XII motoneurons could explain the difference in GAA expression between treatment groups. The GAA transgene product is delivered to lysosomes via receptor-mediated endocytosis.[21,42] This process occurs when a bis-mannose-6-phosphorylated-glycan receptor ligand on the surface of the enzymes binds to the mannose-6-phosphate receptor.[21,42] Recombinant human GAA contains ~0.9–1.2 mol of mannose-6-phosphorylated glycan per mol of enzyme, and of these enzymes only a small proportion have bis-mannose-6-phosphorylated-glycan.[21,42] The lack of receptor ligands reduces the lysosomal uptake of GAA by as much as 1,000-fold, making the process highly inefficient.[15] The IGFIIcoGAA transgene product produced by AAV9-DES-IGFIIcoGAA contains an IGFII-M6P co-receptor ligand, and *in vitro* studies show that this will greatly increase the lysosomal uptake of intracellular GAA.[14] Increased efficiency of lysosomal uptake would in turn result in a greater percentage of XII motoneurons containing a sufficient amount of active GAA enzyme to be visualized immunohistochemically. Additionally, the presence of high levels of the IGFII tag could cause redistribution of the CI-MPR to the plasma membrane and facilitate intercellular uptake of the IGFIIcoGAA transgene product.

In addition to intra-cellular GAA enzyme-trafficking efficiency, intercellular GAA enzyme trafficking efficiency may provide an explanation for the discrepancy in GAA expression between AAV9 treatment groups. Following production of the GAA transgene product, cells may actively secrete the GAA enzyme where it can be taken up by surrounding cells. Evidence for this was provided in a prior histological examination of XII motoneurons following tongue AAV9-GAA treatment. That study provided immunohistochemical examples of robust GAA staining in individual XII motoneurons that were surrounded by clusters of cells with positive GAA staining that was considerably less robust than the neighboring cell.[17] A "cross-correction" of XII motoneurons could potentially occur if GAA secreted from one cell moves via receptor-mediated GAA uptake into an adjacent cell and is subsequently trafficked to lysosomes. It is possible that the efficiency of the processes associated with cross-correction can be enhanced with the fusion of the IGFII tag to the GAA enzyme. For example, if the IGFIIcoGAA fusion protein is secreted by transduced cells, IGFII tag could serve as a ligand for IGFII receptors on cell membranes, allowing for efficient receptor-mediated uptake.[15] In this regard, one consideration is that motoneurons showing pathology after lingual AAV9-GAA therapy may lack the necessary receptors for IGFIIcoGAA uptake, either due to downregulation or degradation.

Significance

The standard of care for patients with Pompe disease is intravenous delivery of rhGAA in a bi-weekly paradigm.[3] This ERT approach can attenuate skeletal muscle pathology,[12] reduce cardiac dilation,[11] and improve the survival rate[11] of early-onset Pompe disease patients. However, ERT does not adequately address neuronal pathology.[43] In fact, by attenuating muscular pathology and preserving muscular function, ERT may reveal a neuronal phenotype in Pompe disease.[44] The limited neuronal impact of ERT likely reflects the fact that intravenously delivered GAA enzyme does not cross the blood brain barrier to treat neuropathology.[3] In addition, inefficient enzyme uptake into neurons could occur due to low cation-independent mannose-6-phosphate receptor density.[14,16,20,37]

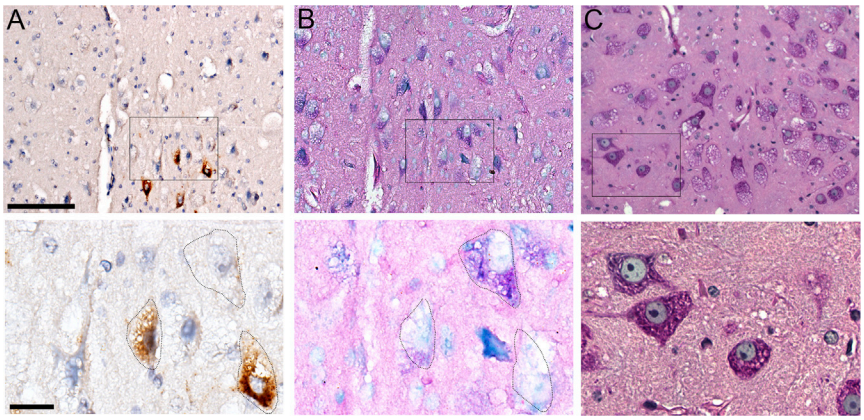

Figure 7. Following AAV Therapy, XII Motoneurons Expressing GAA Do Not Stain for Glycogen

(A) GAA immunostaining in the XII nucleus of a *Gaa*$^{-/-}$ mouse that received a tongue injection with AAV9-DES-coGAA 4 months earlier. Four GAA-positive neurons (brown staining) can be clearly observed; the area indicated by the box is shown at higher magnification in the bottom image. (B) PAS staining from the medullary tissue section immediately adjacent to that shown in (A) (7 μm sections). Comparison of (A) and (B) (bottom images) indicates that cells staining positive for GAA were negative for glycogen (i.e., PAS negative). (C) Photomicrographs of PAS staining in the XII nucleus of an untreated *Gaa*$^{-/-}$ mouse. Scale bars, 100 μm (top panels) and 20 μm (bottom panels).

The respiratory system (including the lingual muscles needed for regulating upper airway patency) appears to be particularly susceptible to neural impairments in Pompe disease.[1] Early onset Pompe patients receiving ERT show neuronal pathology in respiratory neurons[2] and often have progressive respiratory[45] and XII motor dysfunction.[6] Dysfunction in the XII motor system in early-onset patients is evidenced by weak and ineffective swallowing,[21] as well as speech disorders.[6] Adult-onset Pompe disease patients also show lingual weakness, dysphagia, dysarthria, and obstructive sleep apnea despite being treated with ERT.[46,47] These phenotypes are likely to have a neuronal component because they persist after ERT, and preclinical studies in animal models show that XII motoneurons are impaired in Pompe disease.[7,23]

Here we have targeted the lingual motor system, including both myofibers and motoneurons (i.e., the entire motor unit) using intralingual delivery of AAV9 encoding GAA. The results suggest that it will be possible to selectively target lingual dysfunction in Pompe disease using the intralingual delivery approach. Moreover, the increase in the observable number of XII motoneurons expressing GAA in AAV9-DES-IGFIIcoGAA-treated mice suggests that addition of the IGFII GILT tag to GAA may improve the therapeutic efficacy of lingual-directed treatments. Increasing the total number of XII motoneurons expressing GAA after intralingual AAV9-GAA treatment may require multiple injections (e.g., targeting both the anterior and posterior tongue), higher injection volumes and/or AAV titer, or possibly direct AAV injection into the XII nerve trunk.

MATERIALS AND METHODS

Animals

All experimental procedures were approved by the University of Florida Institutional Animal Care and Use Committee (IACUC). 129SVE (WT) mice were obtained from Taconic, Albany, NY. *Gaa*$^{-/-}$ mice were produced by disruption of exon 6 in the *Gaa* gene using a neo cassette (B6;129-Gaa^{tm1Rabn}/J).[48] These mice exhibit weakness beginning at approximately 3 weeks and by 8–9 months show obvious muscle wasting and a weak, waddling gait. *Gaa*$^{-/-}$ mice[16] were outbred to a 129SVE background by Taconic. An intralingual injection of AAV9 vector or LRs was administered at 6 months of age. Animals were weighed prior to injection and then weekly for 4 months following injection. WT, untreated control animals were used for molecular, biochemical, and immunohistological studies and were weighed at 10 months of age prior to tissue harvest. As described subsequently, lingual and brainstem tissues were harvested and processed for molecular, biochemical, and immunohistological studies 4 months post-injection.

AAV Vectors

Single-stranded AAV vectors encoding coGAA, driven by the Desmin promoter, were injected intralingually (1.00e10 vg). This dose was determined by prior experience with tongue injections using AAV9.[17,18] Two AAV9 vectors were used for comparison: AAV9-DES-coGAA, which has been codon optimized for increased translation of the transgene product, and AAV9-DES-IGFIIcoGAA, which has been both codon optimized and engineered to use the IGFII GILT tag to facilitate cellular and lysosomal uptake of the transgene product via the CI-MPR. All vectors were generated and titered at the University of Florida Powell Gene Therapy Center Vector Core Laboratory. Vectors were purified by iodixanol gradient centrifugation and anion-exchange chromatography as described previously.[49] AAV9-DES-coGAA and AAV9-DES-IGFIIcoGAA were diluted to a quantity sufficient volume of 20 μL with LRs solution prior to vector administration.

In Vivo Vector Administration

Animals were treated with the vector at 6 months of age. *Gaa*$^{-/-}$ mice were randomly assigned by blinded investigator to one of three groups: AAV9-DES-coGAA (n = 16), AAV9-IGFIIcoGAA (n = 14), or a sham group (n = 15). WT animals did not receive an injection. Equal numbers of male and female mice were randomly assigned to each group. Mice were anesthetized prior to injection with 3% isoflurane administered in a sealed chamber and then transferred to a nose cone. To maintain body temperature at 37°C, we placed mice on a heating pad during injections. The animal's jaw was opened using blunt forceps, while the tongue was gently retracted using blunt forceps to expose the injection site. A single injection, using a 500 μL, $33^{1}/_{2}$G insulin syringe, of 20 μL of vector in LRs or LRs alone (sham) was delivered to the base of the tongue lateral to the lingual

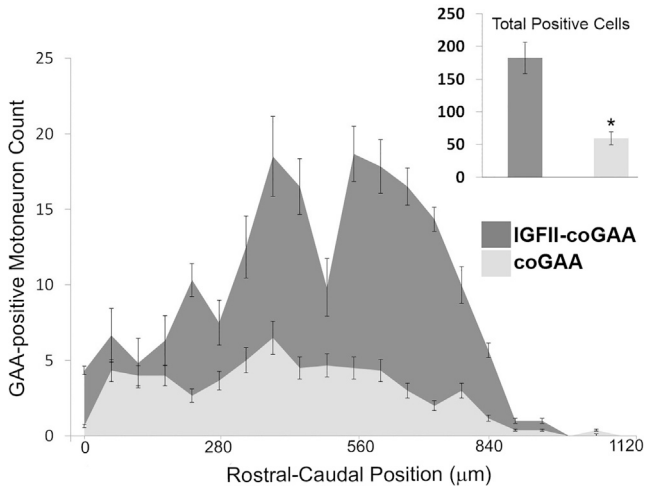

Figure 8. Distribution of GAA-Positive Motoneurons along the Rostral-Caudal Extent of the XII Nucleus following AAV9-GAA Therapy in *Gaa*$^{-/-}$ Mice

The dark gray shading represents AAV9-DES-IGFIIcoGAA (n=7) and the light gray AAV9-DES-coGAA (n=6). In the plot, 0 μm indicates the most rostral point of the XII nucleus. Differences in GAA-positive motoneurons were most apparent in the caudal aspect of the nucleus. The inset panel on the upper right shows the total number of GAA-positive motoneurons, across the entire XII nucleus, in IGFIIcoGAA versus coGAA treated *Gaa*$^{-/-}$ mice (*$p < 0.008$). Error bars indicate SEM.

frenulum. Injection was visually confirmed by localized swelling of the tongue following administration of the fluid bolus. Mice were returned to their original cages following injection. Vector treated and sham animals were kept in separate cages and ear tagged for identification. The animals assigned to the sham group were used as a *Gaa*$^{-/-}$ control group in molecular, biochemical, and histological analyses.

Tongue and Brainstem Histology

Tissues were harvested 4 months post-injection. Mice were deeply anesthetized with 3% isoflurane in a sealed chamber to reach a surgical plane and transferred to a nose cone with continued inspired isoflurane, and then brainstem tissues were harvested immediately and blocked to isolate the medulla. The tongue musculature was harvested next by removal of the lower jaw and cutting of muscular attachment points to remove both intrinsic and extrinsic muscles and blocked into rostral and caudal halves. Medullas and tongues were fixed in Gendre's solution for 24 h. Tissues were then repeatedly washed in 70% ethanol until the solution remained clear and stored in 70% ethanol. The tissues were stained with PAS, H&E, and by immunohistochemical detection of GAA. PAS staining was performed on brainstem and tongue tissues (AAV9-DES-IGFIIcoGAA, n = 6; AAV9-DES-coGAA, n = 7; sham, n = 6) which were first fixed in 10% neutral buffered formalin (NBF), postfixed with 1% periodic acid (PA)/10% NBF, embedded in paraffin, sectioned (7 μm), and mounted in serial and stained with Schiff's reagent.[50] GAA IHC coupled with a Vectastain ABC secondary detection kit and DAB (3,3′-Diaminobenzidine) were performed on mounted sections adjacent to PAS-stained sections (AAV9-DES-IGFIIcoGAA, n = 7; AAV9-DES-coGAA, n = 6; sham, n = 6). The tissue was incubated overnight in primary antibody against GAA, 1:2,000 (rabbit polyclonal GAA antibody (Covance, Emeryville, CA, USA). On the following day, the tissue was washed in PBS, incubated in a biotinylated anti-rabbit immunoglobulin G secondary antibody, 1:200 (Vector Laboratories, Burlingame, CA, USA), and coupled with a Vectastain ABC Kit and DAB for bright-field microscopy. Antibodies were validated by previous studies.[10,18,51]

Automated Three-Dimensional Histological Reconstruction

The tongue of a mouse was reconstructed in three dimensions to assess the distribution of PAS and GAA staining. Custom MATLAB code was used to detect positive staining using L*a*b* color-based segmentation to separate the dark brown in GAA stained sections and dark purple in PAS stained sections. Serial pairs of images (one PAS stained, one GAA stained) spaced 7 μm apart, taken at 4× magnification were registered to each other and across the anterior posterior axis of the tongue using intensity metric optimization. The boundaries of the positively stained regions were then interpolated to form the three-dimensional tongue.

Hypoglossal Nerve Histology

Nerves were processed as described previously.[52] Animals were sacrificed and an approximately 5 mm section of the hypoglossal nerve was harvested, proximal to the bifurcation into lateral and medial branches, for morphological and histological analysis (AAV9-DES-IGFIIcoGAA, n = 6; AAV9-DES-coGAA, n = 7; sham, n = 6). Immediately, post-harvest samples were fixed in 2% glutaraldehyde in 0.2 mol/l Na Cacodylate buffer (pH 7.3) prior to embedding in epon.[53] The epon-embedded nerves were serial sectioned at 1 μm and mounted on glass slides. Following staining with PAS or toluidine blue, sections were qualitatively evaluated by a blinded investigator using light microscopy.

GAA Activity Assay

Following euthanasia, tongue tissues were immediately harvested, frozen in liquid N_2, and maintained at −80°C until biochemical analyses were performed (AAV9-DES-IGFIIcoGAA, n = 7; AAV9-DES-coGAA, n = 8; sham, n = 5; WT, n = 5). Tongue tissues were homogenized in water containing a complete protease inhibitor cocktail (Roche Applied Science, Indianapolis, IN, USA) and subjected to three freeze-thaw cycles. Homogenates were centrifuged at 14,000 rpm for 10 minutes at 4°C and the resulting supernatant was assayed for GAA activity by measuring cleavage of 4-methylumbelliferylα-D-glucopyranoside after incubation for 1 h at 37°C. Protein concentration was measured using the Bio-Rad DC protein assay kit per manufacturer's instructions. Data are expressed in nmol/h/mg of protein.

Microscopy and Quantitative Analyses

Microscopy was done using an Olympus BX43 microscope and an Olympus DP80 camera supported with cellSens imaging software. GAA-positive XII motoneurons with visible nuclei were identified

using bright-field microscopy and counted at 10× magnification in every 6th 7 μm transverse medullary section. Prior to quantification of GAA-positive cells, images were coded to blind the evaluator from the treatment group. XII motoneurons were identified by soma diameter (20–30 μm) and anatomical location. Cells were considered positive when DAB staining was clearly visible throughout the majority of the soma. Cells without a visible nucleus were not counted.

Statistical Analysis

The total number of GAA-positive XII motoneurons was compared, between AAV9-DES-coGAA (n = 6) and AAV9-DES-IGFIIcoGAA (n = 7) injected $Gaa^{-/-}$ mice, using an unpaired t test. Tongue GAA activity data were not normally distributed, and accordingly the groups were compared using Kruskal-Wallis one-way ANOVA on ranks (AAV9-DES-IGFIIcoGAA, n = 7; AAV9-DES-coGAA, n = 8; sham, n = 5; WT, n = 5). Pairwise multiple comparison procedures were conducted using Dunn's Method. Significance was set at $p < 0.05$.

AUTHOR CONTRIBUTIONS

B.M.D., B.J.B., D.J.F., and D.D.F. designed research; B.M.D., S.M.F.T., M.L.J., A.E.P., and L.A.V. performed research; B.M.D., L.A.V., and M.D.S. analyzed data and prepared figures; B.M.D., D.J.F., B.J.B., D.D.F. interpreted and reviewed the data; B.M.D. wrote the initial draft of the manuscript; and B.M.D. and D.D.F. revised and edited the manuscript.

ACKNOWLEDGMENTS

This work was supported by funding from the NIH under grant number 2R01HD052682-06A1 (D.D.F. and B.J.B.). B.M.D. was supported by funding from the University of Florida Graduate School. M.D.S. was supported by F31 HL145831-01 and T32-HD043730. D.J.F. was supported by NIAMS (K01AR066077). We thank Dr. Jonathan LeBowitz at BioMarin Pharmaceutical Inc. for providing the GILT-tag and Dr. Nina Raben for originally providing the $Gaa^{-/-}$ mice.

REFERENCES

1. Fuller, D.D., ElMallah, M.K., Smith, B.K., Corti, M., Lawson, L.A., Falk, D.J., and Byrne, B.J. (2013). The respiratory neuromuscular system in Pompe disease. Respir. Physiol. Neurobiol. *189*, 241–249.

2. DeRuisseau, L.R., Fuller, D.D., Qiu, K., DeRuisseau, K.C., Donnelly, W.H., Jr., Mah, C., Reier, P.J., and Byrne, B.J. (2009). Neural deficits contribute to respiratory insufficiency in Pompe disease. Proc. Natl. Acad. Sci. USA *106*, 9419–9424.

3. Byrne, B.J., Falk, D.J., Pacak, C.A., Nayak, S., Herzog, R.W., Elder, M.E., Collins, S.W., Conlon, T.J., Clement, N., Cleaver, B.D., et al. (2011). Pompe disease gene therapy. Hum. Mol. Genet. *20* (R1), R61–R68.

4. Jones, H.N., Muller, C.W., Lin, M., Banugaria, S.G., Case, L.E., Li, J.S., O'Grady, G., Heller, J.H., and Kishnani, P.S. (2010). Oropharyngeal dysphagia in infants and children with infantile Pompe disease. Dysphagia *25*, 277–283.

5. Margolis, M.L., Howlett, P., Goldberg, R., Eftychiadis, A., and Levine, S. (1994). Obstructive sleep apnea syndrome in acid maltase deficiency. Chest *105*, 947–949.

6. van Gelder, C.M., van Capelle, C.I., Ebbink, B.J., Moor-van Nugteren, I., van den Hout, J.M., Hakkesteegt, M.M., van Doorn, P.A., de Coo, I.F., Reuser, A.J., de Gier, H.H., and van der Ploeg, A.T. (2012). Facial-muscle weakness, speech disorders and dysphagia are common in patients with classic infantile Pompe disease treated with enzyme therapy. J. Inherit. Metab. Dis. *35*, 505–511.

7. Turner, S.M., Hoyt, A.K., ElMallah, M.K., Falk, D.J., Byrne, B.J., and Fuller, D.D. (2016). Neuropathology in respiratory-related motoneurons in young Pompe (Gaa(-/-)) mice. Respir. Physiol. Neurobiol. *227*, 48–55.

8. Mah, C., Pacak, C.A., Cresawn, K.O., Deruisseau, L.R., Germain, S., Lewis, M.A., Cloutier, D.A., Fuller, D.D., and Byrne, B.J. (2007). Physiological correction of Pompe disease by systemic delivery of adeno-associated virus serotype 1 vectors. Mol. Ther. *15*, 501–507.

9. Mah, C.S., Falk, D.J., Germain, S.A., Kelley, J.S., Lewis, M.A., Cloutier, D.A., DeRuisseau, L.R., Conlon, T.J., Cresawn, K.O., Fraites, T.J., Jr., et al. (2010). Gel-mediated delivery of AAV1 vectors corrects ventilatory function in Pompe mice with established disease. Mol. Ther. *18*, 502–510.

10. Falk, D.J., Todd, A.G., Lee, S., Soustek, M.S., ElMallah, M.K., Fuller, D.D., Notterpek, L., and Byrne, B.J. (2015). Peripheral nerve and neuromuscular junction pathology in Pompe disease. Hum. Mol. Genet. *24*, 625–636.

11. Byrne, B.J., Kishnani, P.S., Case, L.E., Merlini, L., Müller-Felber, W., Prasad, S., and van der Ploeg, A. (2011). Pompe disease: design, methodology, and early findings from the Pompe Registry. Mol. Genet. Metab. *103*, 1–11.

12. Van den Hout, J.M., Kamphoven, J.H., Winkel, L.P., Arts, W.F., De Klerk, J.B., Loonen, M.C., Vulto, A.G., Cromme-Dijkhuis, A., Weisglas-Kuperus, N., Hop, W., et al. (2004). Long-term intravenous treatment of Pompe disease with recombinant human alpha-glucosidase from milk. Pediatrics *113*, e448–e457.

13. Schneider, I., Hanisch, F., Müller, T., Schmidt, B., and Zierz, S. (2013). Respiratory function in late-onset Pompe disease patients receiving long-term enzyme replacement therapy for more than 48 months. Wien. Med. Wochenschr. *163*, 40–44.

14. Maga, J.A., Zhou, J., Kambampati, R., Peng, S., Wang, X., Bohnsack, R.N., Thomm, A., Golata, S., Tom, P., Dahms, N.M., et al. (2013). Glycosylation-independent lysosomal targeting of acid α-glucosidase enhances muscle glycogen clearance in pompe mice. J. Biol. Chem. *288*, 1428–1438.

15. Tong, P.Y., and Kornfeld, S. (1989). Ligand interactions of the cation-dependent mannose 6-phosphate receptor. Comparison with the cation-independent mannose 6-phosphate receptor. J. Biol. Chem. *264*, 7970–7975.

16. Raben, N., Danon, M., Gilbert, A.L., Dwivedi, S., Collins, B., Thurberg, B.L., Mattaliano, R.J., Nagaraju, K., and Plotz, P.H. (2003). Enzyme replacement therapy in the mouse model of Pompe disease. Mol. Genet. Metab. *80*, 159–169.

17. ElMallah, M.K., Falk, D.J., Lane, M.A., Conlon, T.J., Lee, K.Z., Shafi, N.I., Reier, P.J., Byrne, B.J., and Fuller, D.D. (2012). Retrograde gene delivery to hypoglossal motoneurons using adeno-associated virus serotype 9. Hum. Gene Ther. Methods *23*, 148–156.

18. Elmallah, M.K., Falk, D.J., Nayak, S., Federico, R.A., Sandhu, M.S., Poirier, A., Byrne, B.J., and Fuller, D.D. (2014). Sustained correction of motoneuron histopathology following intramuscular delivery of AAV in pompe mice. Mol. Ther. *22*, 702–712.

19. Van der Ploeg, A.T., Kroos, M.A., Willemsen, R., Brons, N.H., and Reuser, A.J. (1991). Intravenous administration of phosphorylated acid alpha-glucosidase leads to uptake of enzyme in heart and skeletal muscle of mice. J. Clin. Invest. *87*, 513–518.

20. Yang, H.W., Kikuchi, T., Hagiwara, Y., Mizutani, M., Chen, Y.T., and Van Hove, J.L. (1998). Recombinant human acid alpha-glucosidase corrects acid alpha-glucosidase-deficient human fibroblasts, quail fibroblasts, and quail myoblasts. Pediatr. Res. *43*, 374–380.

21. Zhu, Y., Li, X., McVie-Wylie, A., Jiang, C., Thurberg, B.L., Raben, N., Mattaliano, R.J., and Cheng, S.H. (2005). Carbohydrate-remodelled acid alpha-glucosidase with higher affinity for the cation-independent mannose 6-phosphate receptor demonstrates improved delivery to muscles of Pompe mice. Biochem. J. *389*, 619–628.

22. Elena, C., Ravasi, P., Castelli, M.E., Peirú, S., and Menzella, H.G. (2014). Expression of codon optimized genes in microbial systems: current industrial applications and perspectives. Front. Microbiol. *5*, 21.

23. Lee, K.Z., Qiu, K., Sandhu, M.S., Elmallah, M.K., Falk, D.J., Lane, M.A., Reier, P.J., Byrne, B.J., and Fuller, D.D. (2011). Hypoglossal neuropathology and respiratory activity in pompe mice. Front. Physiol. *2*, 31.

24. McIntosh, P.T., Hobson-Webb, L.D., Kazi, Z.B., Prater, S.N., Banugaria, S.G., Austin, S., Wang, R., Enterline, D.S., Frush, D.P., and Kishnani, P.S. (2018). Neuroimaging

findings in infantile Pompe patients treated with enzyme replacement therapy. Mol. Genet. Metab. *123*, 85–91.

25. Ebbink, B.J., Poelman, E., Aarsen, F.K., Plug, I., Régal, L., Muentjes, C., van der Beek, N.A.M.E., Lequin, M.H., van der Ploeg, A.T., and van den Hout, J.M.P. (2018). Classic infantile Pompe patients approaching adulthood: a cohort study on consequences for the brain. Dev. Med. Child Neurol. *60*, 579–586.

26. Musumeci, O., Marino, S., Granata, F., Morabito, R., Bonanno, L., Brizzi, T., Lo Buono, V., Corallo, F., Longo, M., and Toscano, A. (2019). Central nervous system involvement in late-onset Pompe disease: clues from neuroimaging and neuropsychological analysis. Eur. J. Neurol. *26*, 442–e35.

27. Allen Institute for Brain Science (2015). Allen Human Brain Atlas API. http://help.brain-map.org/display/api/Allen%2BBrain%2BAtlas%2BAPI.

28. Falk, D.J., Soustek, M.S., Todd, A.G., Mah, C.S., Cloutier, D.A., Kelley, J.S., Clement, N., Fuller, D.D., and Byrne, B.J. (2015). Comparative impact of AAV and enzyme replacement therapy on respiratory and cardiac function in adult Pompe mice. Mol. Ther. Methods Clin. Dev. *2*, 15007.

29. Mah, C., Cresawn, K.O., Fraites, T.J., Jr., Pacak, C.A., Lewis, M.A., Zolotukhin, I., and Byrne, B.J. (2005). Sustained correction of glycogen storage disease type II using adeno-associated virus serotype 1 vectors. Gene Ther. *12*, 1405–1409.

30. Foust, K.D., Nurre, E., Montgomery, C.L., Hernandez, A., Chan, C.M., and Kaspar, B.K. (2009). Intravascular AAV9 preferentially targets neonatal neurons and adult astrocytes. Nat. Biotechnol. *27*, 59–65.

31. Kaspar, B.K., Lladó, J., Sherkat, N., Rothstein, J.D., and Gage, F.H. (2003). Retrograde viral delivery of IGF-1 prolongs survival in a mouse ALS model. Science *301*, 839–842.

32. Samaranch, L., Salegio, E.A., San Sebastian, W., Kells, A.P., Foust, K.D., Bringas, J.R., Lamarre, C., Forsayeth, J., Kaspar, B.K., and Bankiewicz, K.S. (2012). Adeno-associated virus serotype 9 transduction in the central nervous system of nonhuman primates. Hum. Gene Ther. *23*, 382–389.

33. Sturrock, R.R. (1991). Stability of motor neuron and interneuron number in the hypoglossal nucleus of the ageing mouse brain. Anat. Anz. *173*, 113–116.

34. Clarkson, A.N., Talbot, C.L., Wang, P.Y., MacLaughlin, D.T., Donahoe, P.K., and McLennan, I.S. (2011). Müllerian inhibiting substance is anterogradely transported and does not attenuate avulsion-induced death of hypoglossal motor neurons. Exp. Neurol. *231*, 304–308.

35. Fortun, J., Puzis, R., Pearse, D.D., Gage, F.H., and Bunge, M.B. (2009). Muscle injection of AAV-NT3 promotes anatomical reorganization of CST axons and improves behavioral outcome following SCI. J. Neurotrauma *26*, 941–953.

36. McHanwell, S., and Biscoe, T.J. (1981). The sizes of motoneurons supplying hindlimb muscles in the mouse. Proc. R. Soc. Lond. B Biol. Sci. *213*, 201–216.

37. Gestreau, C., Dutschmann, M., Obled, S., and Bianchi, A.L. (2005). Activation of XII motoneurons and premotor neurons during various oropharyngeal behaviors. Respir. Physiol. Neurobiol. *147*, 159–176.

38. Castle, M.J., Perlson, E., Holzbaur, E.L., and Wolfe, J.H. (2014). Long-distance axonal transport of AAV9 is driven by dynein and kinesin-2 and is trafficked in a highly motile Rab7-positive compartment. Mol. Ther. *22*, 554–566.

39. Castle, M.J., Gershenson, Z.T., Giles, A.R., Holzbaur, E.L., and Wolfe, J.H. (2014). Adeno-associated virus serotypes 1, 8, and 9 share conserved mechanisms for anterograde and retrograde axonal transport. Hum. Gene. Ther. *25*, 705–720.

40. Mitrabhakdi, E., Shuangshoti, S., Wannakrairot, P., Lewis, R.A., Susuki, K., Laothamatas, J., and Hemachudha, T. (2005). Difference in neuropathogenetic mechanisms in human furious and paralytic rabies. J. Neurol. Sci. *238*, 3–10.

41. Finke, S., and Conzelmann, K.K. (2005). Replication strategies of rabies virus. Virus Res. *111*, 120–131.

42. McVie-Wylie, A.J., Lee, K.L., Qiu, H., Jin, X., Do, H., Gotschall, R., Thurberg, B.L., Rogers, C., Raben, N., O'Callaghan, M., et al. (2008). Biochemical and pharmacological characterization of different recombinant acid alpha-glucosidase preparations evaluated for the treatment of Pompe disease. Mol. Genet. Metab. *94*, 448–455.

43. Byrne, B.J., Fuller, D.D., Smith, B.K., Clement, N., Coleman, K., Cleaver, B., Vaught, L., Falk, D.J., McCall, A., and Corti, M. (2019). Pompe disease gene therapy: neural manifestations require consideration of CNS directed therapy. Ann. Transl. Med. *7*, 290.

44. Chan, J., Desai, A.K., Kazi, Z.B., Corey, K., Austin, S., Hobson-Webb, L.D., Case, L.E., Jones, H.N., and Kishnani, P.S. (2017). The emerging phenotype of late-onset Pompe disease: A systematic literature review. Mol. Genet. Metab. *120*, 163–172.

45. Chakrapani, A., Vellodi, A., Robinson, P., Jones, S., and Wraith, J.E. (2010). Treatment of infantile Pompe disease with alglucosidase alpha: the UK experience. J. Inherit. Metab. Dis. *33*, 747–750.

46. Dubrovsky, A., Corderi, J., Lin, M., Kishnani, P.S., and Jones, H.N. (2011). Expanding the phenotype of late-onset Pompe disease: tongue weakness: a new clinical observation. Muscle Nerve *44*, 897–901.

47. Boentert, M., Dräger, B., Glatz, C., and Young, P. (2016). Sleep-Disordered Breathing and Effects of Noninvasive Ventilation in Patients with Late-Onset Pompe Disease. J. Clin. Sleep Med. *12*, 1623–1632.

48. Raben, N., Nagaraju, K., Lee, E., Kessler, P., Byrne, B., Lee, L., LaMarca, M., King, C., Ward, J., Sauer, B., and Plotz, P. (1998). Targeted disruption of the acid alpha-glucosidase gene in mice causes an illness with critical features of both infantile and adult human glycogen storage disease type II. J. Biol. Chem. *273*, 19086–19092.

49. Zolotukhin, S., Potter, M., Zolotukhin, I., Sakai, Y., Loiler, S., Fraites, T.J., Jr., Chiodo, V.A., Phillipsberg, T., Muzyczka, N., Hauswirth, W.W., et al. (2002). Production and purification of serotype 1, 2, and 5 recombinant adeno-associated viral vectors. Methods *28*, 158–167.

50. Taksir, T.V., Griffiths, D., Johnson, J., Ryan, S., Shihabuddin, L.S., and Thurberg, B.L. (2007). Optimized preservation of CNS morphology for the identification of glycogen in the Pompe mouse model. J. Histochem. Cytochem. *55*, 991–998.

51. Doerfler, P.A., Todd, A.G., Clément, N., Falk, D.J., Nayak, S., Herzog, R.W., and Byrne, B.J. (2016). Copackaged AAV9 Vectors Promote Simultaneous Immune Tolerance and Phenotypic Correction of Pompe Disease. Hum. Gene Ther. *27*, 43–59.

52. Fu, H., DiRosario, J., Kang, L., Muenzer, J., and McCarty, D.M. (2010). Restoration of central nervous system alpha-N-acetylglucosaminidase activity and therapeutic benefits in mucopolysaccharidosis IIIB mice by a single intracisternal recombinant adeno-associated viral type 2 vector delivery. J. Gene Med. *12*, 624–633.

53. Auld, D.S., and Robitaille, R. (2003). Perisynaptic Schwann cells at the neuromuscular junction: nerve- and activity-dependent contributions to synaptic efficacy, plasticity, and reinnervation. Neuroscientist *9*, 144–157.